Density-Functional Theory Study of Iron(III) Hydrolysis in Aqueous Solution

Heitor Avelino De Abreu, Luciana Guimarães, and Hélio Anderson Duarte*

Grupo de Pesquisa em Química Inorgânica Teórica, Departamento de Química, ICEx, Universidade Federal de Minas Gerais, Belo Horizonte, MG, 31.270-901, Brazil

Received: February 2, 2006; In Final Form: March 24, 2006

Fe(III) hydrolysis in aqueous solution has been investigated using density-functional methods (DFT). All possible structures arising from different tautomers and multiplicities have been calculated. The solvation energy has been estimated using the UAHF−PCM method. The hydrolysis free energies have been estimated and compared with the available experimental data. The different hydrolysis species have distinct geometries and electronic structures. We have shown that improvement of theory level in calculating the electronic energy does not necessarily improve the estimated free energies in aqueous solution since the UAHF−PCM is a simple method that neglects specific interactions with the solvent. Therefore, it is important to have the correct balance between theory level used in the electronic calculation and the UAHF−PCM. The PBE/TZVP/UAHF−PCM method has been found to describe correctly the hydrolysis energies of Fe(III), deviating about 3.0 kcal mol^{-1} from experimental values.

1. Introduction

Hydration and hydrolysis of metal ions in aqueous solution play a fundamental role in the reactivity and mobility of these species in aquatic environment[1] and biological[2] systems. Despite the progress in the recent years, current instrumental methods are still far from being able to determine microstructures and stoichiometry of different species arising from hydration and hydrolysis of metal ions. The study of these species at the molecular level is the first step to understanding the chemical, biological, and surface reactivity of metal ions.

Fe(III) is one of these metal ions that are important in many different processes related to biology,[3] environment,[4,5] and catalysis.[6] Formation of different species by hydrolysis gives rise to a complex equilibrium in solution as pH increases. $[Fe(OH)_x(H_2O)_m]^{3-x}$ species are formed; however, the favorable geometries, isomers, and conformations are difficult to be determined. The number of water molecules in the first sphere of solvation has to be determined. These factors must be taken into account for the understanding of the Fe(III) adsorption mechanism on the mineral and its mobility in the environment. The electronic structures of these species are also important in understanding the catalytic effect of iron(III) in the oxidation of pyrite at high pH.[7,8] Innersphere electron transfer between the iron(III) species and the pyrite surface can involve electronically excited states of these species;[9] therefore, a theoretical investigation of Fe(III) hydrolysis can be helpful to improve our knowledge on iron(III) species in aqueous solutions.

Density-functional theory (DFT) calculations have been successfully applied to study metal ions in solution.[10−12] Most of the theoretical studies in this field are based on hydrated ions,[10,11] and only a little attention has been given to the hydrolyzed species[12] which are much more complex. In the present work, we have studied all conformations, isomers, and geometries of the $[Fe(OH)_x(H_2O)_m]^{3-x}$ ($x = 0, 4$) species and their low lying excited states through DFT calculations. The stepwise hydrolysis equilibrium constants have been estimated and compared with the available experimental values.

2. Computational Details

Density-Functional Calculations. All calculations were performed using the linear combination of Gaussian-type orbitals−Kohn−Sham density functional (LCGTO-KS-DFT) method implemented in deMon[13] program package. The following generalized gradient approximations (GGA) for the exchange and correlation (XC) functional have been used: BP86 scheme with the Becke[14] expression for exchange and Perdew[15] expression for correlation, and PBE scheme with Perdew, Burke, and Ernzerhof[16] expression for exchange and correlation. We have used the DZVP and TZVP basis sets optimized explicitly for DFT by Godbout et al.[17] and the Ahlrichs basis sets (A-PVTZ).[18] Automatically generated auxiliary basis sets (A2) have been used for fitting the charge density. Adaptive grid[19,20] with a tolerance of 10^{-6} for the numerical integration of the exchange-correlation and potential energy was used. All structures have been fully optimized without symmetry constraint using the standard Broyden−Fletcher−Goldfarb−Shanno (BFGS)[21−25] method. Harmonic frequency calculations have been performed. The Hessian matrix was evaluated numerically from the analytical gradients of the energy. Positive frequencies ensure that a true minimum on the potential energy surface has been found. The thermodynamic properties at gas phase have been evaluated using the canonical formalism[26] at 298 K.

Solvation Model. Nonspecific solvent effects have been estimated using the united atoms Hartree−Fock/polarizable continuum model (UAHF/PCM).[27,28] The solvation energies have been estimated using the Gaussian 98[29] program package. As described by Saracino et al.,[30,31] we have used for all calculations the UAHF radii obtained by single point calculations at the HF/6-31G(d,p) level of theory using DFT optimized structures in gas phase. In the UAHF/PCM approach the solute is placed in a polarizable cavity formed of spheres centered in the atomic groups. Inside the cavity, the dielectric constant is the same in a vacuum, and outside it takes the solvent value ($\epsilon = 78.4$ for water).

* To whom correspondence should be addressed. E-mail: duarteh@ufmg.br. Phone: ++55-31-3499-5748. Fax: ++55-31-3499-5700.

10.1021/jp060714h CCC: $33.50
Published on Web 05/25/2006

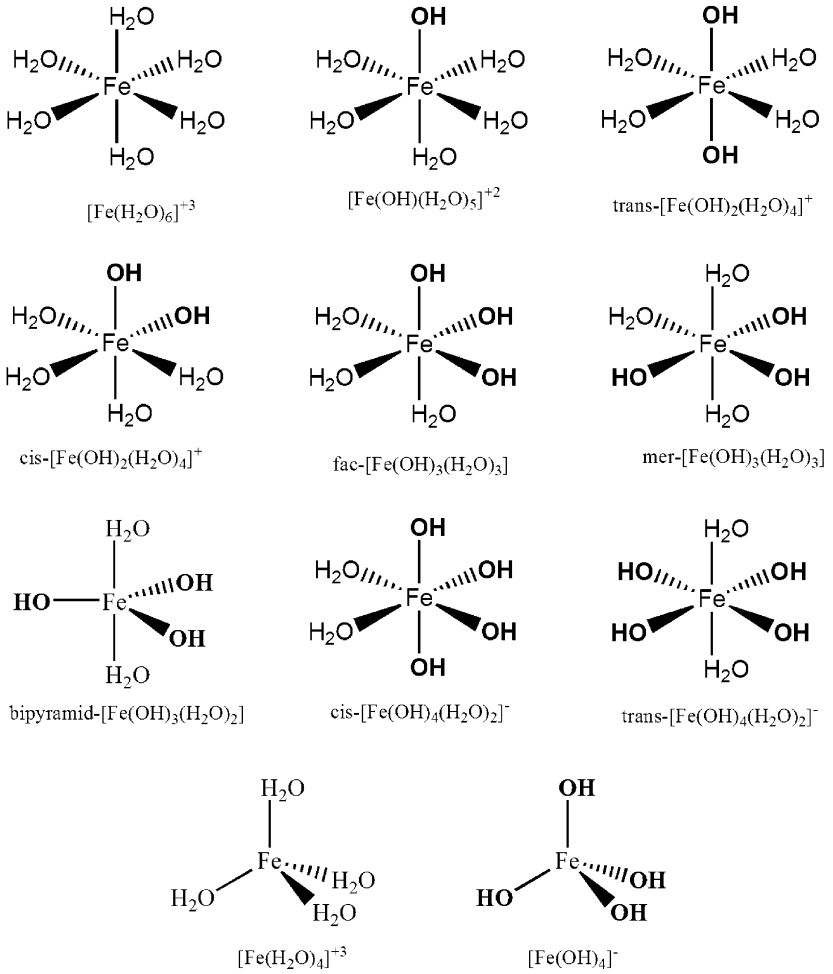

Figure 1. Initial structures used to perform geometry optimization.

Initial Guess Species. The Fe(III) hydrolysis products, $[Fe(OH)_x]^{3-x}$ ($x = 0-4$) complexes, have been investigated in an attempt to contribute to the understanding of Fe(III) speciation in aqueous solution at a molecular level. Different multiplicities arising from the excitation of the partially occupied Fe d shell of all possible isomers, conformations, and structures have been calculated exploring the whole potential-energy surface. Harris and co-workers[10] showed that DFT can yield reasonable aqueous iron(III) ground-state structures and also the excited-state properties. It is possible to simulate the distribution of the species with respect to pH; however, information about their geometries and electronic structures are difficult to be gathered on the sole basis of experimental studies. In the present work, the Fe(III) first sphere of coordination was filled with water molecules in such a way that all structures used as starting geometries for the optimization had coordination number 6, as shown in Figure 1.

3. Results and Discussion

$[Fe(H_2O)_6]^{3+}$. Hexaaquairon(III) has been theoretically and experimentally studied quite extensively.[10,11,32−39] The octahedral geometry with weak-field water ligands leads, according to ligand field theory, to the break of degeneracy of the d shell, and the sextet ground state has the valence electronic configuration $t_{2g}^3e_g^2$. The Fe−O distances experimentally determined by different methods are in the range of 1.97−2.05 Å.[36,40] Ohtaki and Radnai discuss in their review[38] a number of experiments and concluded that the Fe−O distance lies in the range of 2.01−2.05 Å. The optimized geometry of the $[Fe(H_2O)_6]^{3+}$ is shown in Figure 2a. The predicted structural parameters are in good agreement with the previously published results.[11,12,37,41−44] Harris et al. have predicted the Fe−O distances to be about 2.08 Å using the BPW91/A-PVTZ level of theory which should be compared with our results of 2.067 Å for PBE/TZVP. This result supports the observation that in such systems in which the electronic correlation effects are important, the Fe−O bond distances can differ by about 0.02 Å depending on the XC scheme used. The UMP2/A-PVTZ Fe−O bond distance is predicted to be 2.06 Å, 0.01 Å smaller than our DFT value. The doublet and quartet low-lying excited states are predicted to be about 15.8 and 20.3 kcal mol^{-1} (see Table 1) higher in energy than the sextet ground state at the BP86/DZVP level of theory. These values may be compared with the previously published BPW91 and BLYP results[10] which predicted the values of 22.3 and 25.6 kcal mol^{-1} for the sextet−quartet gap, respectively, and 20.6 and 22.7 kcal mol^{-1} for the sextet−doublet gap, respectively.

$[Fe(OH)(H_2O)_5]^{2+}$. The $[Fe(OH)(H_2O)_5]^{2+}$ optimized structure is shown in Figure 2b. The Fe−OH bond distance is predicted to be 1.764 Å and Fe−OH_2 bond distances are predicted to be in the range of 2.100−2.162 Å. Martin and co-workers,[12] using the B3LYP/6-31G* hybrid functional, found the Fe−OH distance equal to 1.760 Å and Fe−OH_2 distances lengthening to 2.103−2.150 Å, which are in very good agreement with our results. Another work done by Li et al.[45] have studied this hydroxo species with one and two solvent coordination shells using the BP86/TZVP method. The Fe−OH distance in the solvated system was predicted to be equal

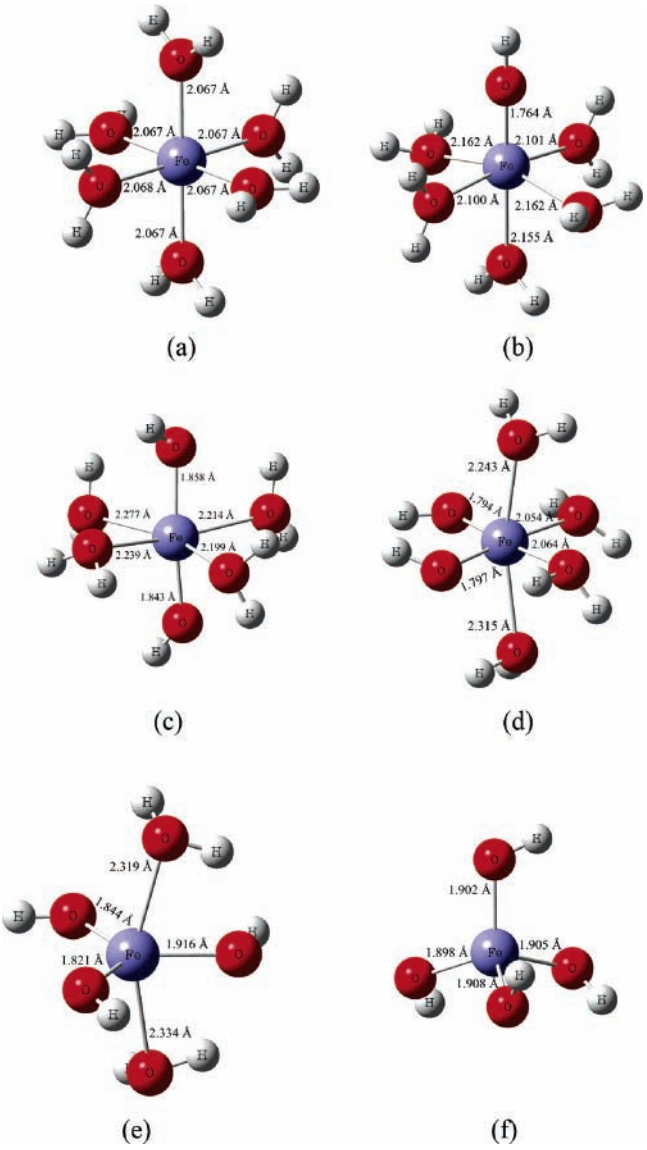

Figure 2. The most stable structures arising from the hydrolysis of Fe(III). Fe−O bond distances are shown.

TABLE 1: Relative Energies of the Different Species at the BP86/DZVP Level of Theory

	2S + 1		
species	2	4	6
$[Fe(H_2O)_6]^{3+}$	20.3	15.8	0.0
$[Fe(OH)\ (H_2O)_5]^{2+}$	10.2	5.9	0.0
cis-$Fe(OH)_2\ (H_2O)_4]^{+}$	4.9	0.0	1.0
bipyramid $[Fe(OH)_3\ (H_2O)_2]$	16.9	0.3	0.0
$[Fe(OH)_4]^{-}$	20.0	3.6	0.0

to 1.787 Å, which is in agreement with the values found in our work. It is important to note the influence exerted by the water molecules of the second coordination shell which leads to the increase of the Fe−O bond distances. The doublet and quartet electronic states lie 10.2 and 5.9 kcal mol^{-1} higher in energy than the sextet ground state at the BP86/DZVP level of theory (see Table 1).

$[Fe(OH)_2(H_2O)_4]^{+}$. The second deprotonation process produces two different species the *trans*- and *cis*-$[Fe(OH)_2\ (H_2O)_4]^{+}$. The cis isomer is the most stable species being about 5 kcal mol^{-1} lower in energy than the trans isomer. The cis ground-state species is a quartet and the sextet state lies only 1 kcal mol^{-1} higher in energy. The replacement of water ligands to weaker-field ligands OH^{-} breaks the octahedral symmetry, and consequently, different states as quartet can become more stable. The *cis*-$[Fe(OH)_2(H_2O)_4]^{+}$ species is shown in Figure 2d, which presents Fe−OH and Fe−OH_2 bond distances predicted to be 1.794 and 2.054−2.315 Å, respectively. In an earlier study, Martin[12] found Fe−OH distances equal to 1.820 Å and 1.847 Å, and the Fe−OH_2 distances are in the range of 2.172−2.296 Å. The Fe−OH_2 distances are in the same range as our values and the Fe−OH distances are larger by about 0.026 Å. Kubicki[41] has also studied this species. He found a stable octahedral species only when using a supermolecule model with 10 water molecules surrounding the solvated complex. Their Fe−OH and Fe−OH_2 bond distances are predicted to be 1.80 and 2.11 Å, respectively, using B3LYP/6-311G(d). Even though he has performed this study with a second solvation shell, it is important to note that his results support our Fe^{3+} hydrolysis model.

Concerning the trans isomer (Figure 2c), the sextet species is the ground state and lies about 0.1 kcal mol^{-1} higher in energy than the quartet one. It is interesting to note the presence of the trans effect evidenced by the lengthening of the Fe−OH bonds which are predicted to be 1.843 Å. One can compare these distances with that present in the $[Fe(H_2O)_5(OH)]^{2+}$ species, that is about 0.079 Å shorter. Two different works[12,46] show the same Fe−OH bond distances equal to 1.851 Å. That is in very good agreement with our results.

Using 10 water molecules in a supermolecule model, Kubicki[41] found a difference between the isomeric species equal to 4.8 kcal mol^{-1}, in good agreement with our results. However, it is important to note that, in the supermolecule model, water molecules are added forming a second solvation shell which can lead to artifacts since the dynamical behavior of the solvent is not included in such a model. The water molecule or hydroxyl ion bound to the Fe center can be rich or deficient of hydrogen bonding depending how water molecules of the second shell are placed, and, consequently, the Fe−O bond distances can increase or decrease.

$[Fe(OH)_3(H_2O)_2]$. The *fac*-$[Fe(H_2O)_3(OH)_3]$ and *mer*-$[Fe(H_2O)_3(OH)_3]$ species are not minima in the potential-energy surface. The optimized structure is pentacoordinated presenting trigonal bipyramid geometry. The remaining water molecule is not bonded to the Fe atom. The OH^{-} ligands prefer to stay in the equatorial positions, and H_2O ligands are bonded at axial positions. It is important to note that the axial axis is distorted presenting an angle of 75.3° with respect to the equatorial plane formed by the OH^{-} groups (Figure 2e). According to previous data obtained by Kubicki,[41] considering the second shell of solvation with eight water molecules, the average value for the Fe−OH distances is equal to 1.89 Å, which may be compared to our average value of 1.86 Å.

The sextet ground state lies about 0.3 and 16.9 kcal mol^{-1} lower in energy than the quartet and doublet electronic states, respectively, at the BP86/DZVP level of theory (see Table 1). Other possible structures can be envisaged for the $[Fe(OH)_3]$ complex in aqueous solution. The tetrahedral geometry, with one water ligand bonded to the iron center, is also possible. To determine which species is the preferred one in aqueous medium, we have calculated the reaction free energy described at

$$[Fe(H_2O)_2(OH)_3] \rightleftharpoons [Fe(H_2O)(OH)_3] + H_2O \qquad (1)$$

At the BP86/DZVP level of theory, the ΔE^{elec}, ΔG^{therm}, and ΔG^{solv} are estimated to be 5.7, 16.1, and −9.3 kcal mol^{-1}, respectively, leading to ΔG_{aq}^{tot} equal to 12.5 kcal mol^{-1}. This

TABLE 2: Reaction Free Energies of the Fe(III) Hydrolysis Using Different Levels of Theory[a,b]

reactions	basis sets	ΔE_e	$\Delta G^{T\,c}$	ΔG^{solv}	$\Delta G^{tot\,d}$	$-\log \beta$
$[Fe(H_2O)_6]^{3+} + H_2O \rightarrow [Fe(OH)(H_2O)_5]^{2+} + H_3O^+$	BP86/DZVP	−151.4	4.8	143.6	−5.3	−3.9
	BP86/A-PVTZ	−145.7		144.4	1.2	0.9
	BP86/TZVP	−145.0		152.5	9.9	7.2
	PBE/DZVP	−150.0		146.3	−1.3	−0.9
	PBE/A-PVTZ	−145.5		147.0	3.9	2.9
	PBE/TZVP	−147.8		147.0	1.6	1.2
	exptl				3.0	2.2
$[Fe(H_2O)_6]^{3+} + 2H_2O \rightarrow [Fe(OH)_2(H_2O)_4]^+ + 2H_3O^+$	BP86/DZVP	−190.1	15.4	174.3	−5.2	−3.8
	BP86/A-PVTZ	−173.5		181.0	18.2	13.3
	BP86/TZVP	−174.7		178.1	14.0	10.3
	PBE/DZVP	−187.6		179.5	2.5	1.9
	PBE/A-PVTZ	−172.8		177.4	15.3	11.2
	PBE/TZVP	−184.9		179.3	5.0	3.7
	exptl				7.8	5.7
$[Fe(H_2O)_6]^{3+} + 2H_2O \rightarrow [Fe(OH)_3(H_2O)_2] + 3H_3O^+$	BP86/DZVP	−114.3	8.0	113.1	2.0	1.4
	BP86/A-PVTZ	−101.3		122.4	24.3	17.8
	BP86/TZVP	−105.0		124.3	22.5	16.5
	PBE/DZVP	−112.4		123.3	14.2	10.4
	PBE/A-PVTZ	−98.8		124.8	29.2	21.4
	PBE/TZVP	−110.1		123.6	16.8	12.3
	exptl				18.5	13.6
$[Fe(H_2O)_6]^{3+} + 2H_2O \rightarrow [Fe(OH)_4]^- + 4H_3O^+$	BP86/DZVP	55.9	5.9	−38.6	18.5	13.6
	BP86/A-PVTZ	69.1		−29.2	41.0	30.1
	BP86/TZVP	61.7		−27.6	35.3	25.8
	PBE/DZVP	56.6		−28.9	28.8	21.1
	PBE/A-PVTZ	73.9		−27.4	47.6	34.9
	PBE/TZVP	58.7		−28.1	31.8	23.3
	exptl				29.5	21.6

[a] All energies are in kcal mol^{-1}. [b] Medium used in PCM model is water ($\epsilon = 78.4$). [c] Thermal contribution at 298 K. The zero-point energy is included. [d] $\Delta G^{tot} = \Delta E_e + \Delta G^T + \Delta G^{solv} - nRT \ln[H_2O]$.

means that the pentacoordinated bipyramid structure is favored in aqueous solution.

$[Fe(OH)_4]^-$. The *cis*- and *trans*-$[Fe(H_2O)_2(OH)_4]^-$ are also not minima in the potential energy surface, and both converged to the tetrahedral form $[Fe(OH)_4]^-$ (Figure 2f). In contrast to octahedral species predicted by hydrolysis data,[47] we found a tetrahedral form to be the most stable species. We can compare our geometrical parameters with those calculated early by Kubicki[41] that studied a very similar species, $[Fe(OH)_4(H_2O)_2]^-$, being the water molecules in the first solvation shell and having specific interactions with the OH^- groups. In this way he found the medium distances Fe−OH to be equal to 1.88 Å. Our values are again longer than those by less than 0.02 Å, and this deviance is probably due to both the XC scheme used and the specific interactions considered by Kubicki in his work.

p*Ka* Estimate. Hexaaquairon(III) is an acid which deprotonates according to the solution pH. The many hydrolysis species formed in the medium are the blocks to form the polynuclear hydroxylated species of iron(III). The pK_a values of $[Fe(H_2O)_6]^{3+}$ allow us to simulate the species distribution with respect to the pH; however, information concerning electronic and geometrical structure of these species is difficult to investigate. It has been shown that theoretically estimated reaction energies of the deprotonation process follow the correct trends and correlate with the equilibrium constants reasonably well.[39,41] It is important to correctly determine the predominant species and their solvation energies. The treatment of the proton solvation is still a challenge, even though the simple H_3O^+ model seems to work reasonably well.[48,49] Most of the theoretical pK_a estimates have been performed for closed shell systems as carboxylic acids[49−53] and other organic systems.[48,54,55] Despite this effort, it is still necessary to show the reliability of this method for open shell systems.

Concerning the hydrolysis of Fe^{3+}, Li et al.[45] have calculated the first pK_a using the BP86/TZVP level of theory. The pK_a estimate of −4.0 deviated significantly from the experimental value of 2.2. Rustad and co-workers[39] showed that DFT calculated hydrolysis energies have good correlation with the observed first pK_a of aqueous trivalent ions. Kubicki[41] extended the study to the successive pK_a values showing that correlations of deprotonation energies with observed pK_a values follow the expected behavior for individual Al^{3+}, Fe^{3+}, and Si^{4+} cations. However, the linear free energy relationship for Fe(III) hydrolysis leads to a slope that corresponds to 481 K, which is too high. This corresponds to an error of 50 kcal mol^{-1} in the fourth hydrolysis constant ($-\log(\beta) = 21.6$). He pointed out four factors for this disagreement:[41] inadequate method, model structures which do not reflect the aqueous Fe(III) species, Fe(III) complexes in solution, or uncertainties in the log β for Fe(III) hydrolysis.

The four pK_a values of the $[Fe(H_2O)_6]^{3+}$ observed experimentally are 2.2, 3.5, 6.3, and 9.6.[46,56] The energetics is adequately described using the following equations:

$$[Fe(H_2O)_6]^{3+} + H_2O \rightleftharpoons [Fe(H_2O)_5(OH)]^{2+} + H_3O^+ \qquad -\log(\beta) = 2.2 \quad (2)$$

$$[Fe(H_2O)_6]^{3+} + 2H_2O \rightleftharpoons [Fe(H_2O)_4(OH)_2]^+ + 2H_3O^+ \qquad -\log(\beta) = 5.7 \quad (3)$$

$$[Fe(H_2O)_6]^{3+} + 2H_2O \rightleftharpoons [Fe(H_2O)_2(OH)_3] + 3H_3O^+ \qquad -\log(\beta) = 13.4 \quad (4)$$

$$[Fe(H_2O)_6]^{3+} + 2H_2O \rightleftharpoons [Fe(OH)_4]^- + 4H_3O^+ \qquad -\log(\beta) = 21.6 \quad (5)$$

The Fe(III) hydrolysis deprotonation energies have been estimated using the thermodynamic cycle shown in Figure 3. To compare this value with the experimental values for the reaction of eqs 2−5, one has to add a correction because water is a

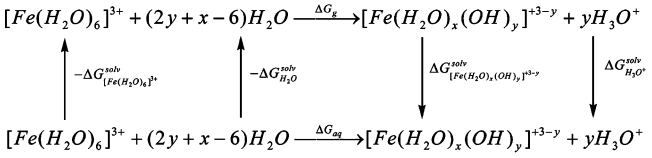

Figure 3. Thermodynamic cycle used to estimate the hydrolysis reaction energies.

reactant, according to eq 6.[57]

$$\Delta G^{\mathrm{Corr}} = \Delta G_{\mathrm{aq}} - nRT \ln(a_{\mathrm{H_2O}}) \qquad (6)$$

The a_{H_2O} was approximated to the ideal solution limit, that is, $a_{H_2O} \approx [H_2O]$. The $[H_2O]$ equal to 55.5 mol L^{-1} has been used leading to a correction of $-2.38n$ kcal mol^{-1}, in which n is the number of water molecules acting as reactant.

It is worthwhile to separate the reaction free energies in each contribution according to eq 7.

$$\Delta G^{\mathrm{tot}}_{\mathrm{aq}} = \Delta E^{\mathrm{elect}}_{\mathrm{g}} + \Delta G^{\mathrm{therm}} + \Delta G^{\mathrm{solv}} \qquad (7)$$

All energy estimates and the respective equilibrium constants are shown in Table 2. The estimate of equilibrium constants of reactions in condensed medium is a very difficult task. It has been pointed out by De Abreu et al.[48] that DFT calculated thermal contribution is insensitive to the choice of XC functional and basis sets. They showed that the difference is not larger than 1 kcal mol^{-1}. Therefore, we decided to calculate this contribution at the level of BP86/DZVP. The UAHF/PCM method has limitations as any other method based in the continuum models for estimating solvation energy. Specific interaction of the solvent with the solute is not taken into account in this type of model. However, in the literature there are enough evidences that these specific interactions are canceled when the reaction involves similar reactants and products.[30,51,54] In fact it is not easy to establish a manner to improve the results in order to estimate experimental equilibrium constants and free reaction energies in aqueous solution. However, it has been speculated that a great part of the success of estimating equilibrium constant values is due to a good synergism between level of theory, basis sets, and the continuum method leading to error compensation.[48] For open shell systems, it is important to ensure that the converged electronic density is free of spin contamination, since this can significantly interfere in the solvation energy estimated by the UAHF/PCM. Therefore we have used the restricted open shell Hartree−Fock (ROHF) method for calculating the open-shell systems.

According to Table 2, the solvation energy has the same magnitude as the electronic energy. Hence, it is an important contribution that can favor or not a specific reaction. Therefore, the good balance between the theoretical method that calculates the electronic energy and the UAHF/PCM model for solvation energy is important. It is observed that slight differences in the geometry can change the solvation energy estimates up to 10 kcal mol^{-1}. This is particularly true when the DZVP and TZVP basis sets results are compared. The compacted A-PVTZ basis sets do not follow the same trends as the other basis sets with respect to the electronic energy. For all reactions studied, the PBE XC functional performs much better compared to the BP86 scheme. PBE results are closer to the experimental values. It is important to note that PBE describes better weak interactions such as those related to the hydrolysis of Fe(III) species.[58]

In Figure 4, the experimental $-\log(\beta)$ is plotted against the estimated hydrolysis free energies. The successive reaction

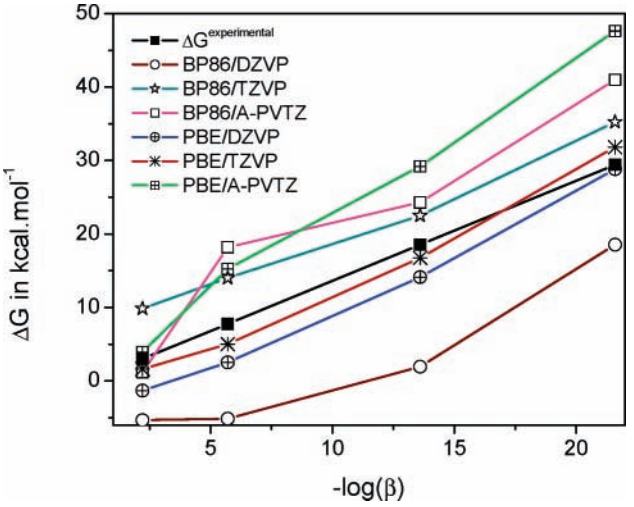

Figure 4. Comparison between the theoretically estimated Gibbs free energy of Fe(III) hydrolysis and the respective experimental value.

energies must lie in a straight line according to the thermodynamics. The BP86/DZVP does not follow a line as it is expected. However, the other methods follow the same tendency having different shifts with respect to the experimental values. It can be observed that the PBE/TZVP provides the results that are closest to the experimental line with error bars about 3 kcal mol^{-1}. It is important to note that we are neglecting the ionic strength of the solution, and also that the error bar of the experimental free energies quoted from the experimental hydrolysis constants are normally about 1 logarithmic unit, that is, about 1.4 kcal mol^{-1}.

Final Remarks. The geometrical, electronic, and thermodynamic properties of Fe(III) species arising from its hydrolysis in aqueous solution have been reported. High-spin ground state is favored for all species as it is expected. The solvation energy estimate is very important since it accounts roughly for a half of the reaction energy. However, continuum methods as the UAHF−PCM are based in simple models and cannot be improved easily. Therefore, the use of such an approach has to be combined with a method for the electronic calculations that provides the best results. Simply increasing the level of theory does not ensure that one is improving the reaction free energy in solution using the thermodynamic cycle of Figure 1. While the gas-phase reaction free energy can be improved, in the aqueous solution one has to face the challenge of calculating the solvation energy of the reactants. In our approach, the PBE/TZVP/UAHF−PCM provided the best results for all hydrolysis reactions studied following the expected behavior. The PBE/TZVP/UAHF−PCM estimated hydrolysis reaction energies are about 3.0 kcal mol^{-1} different from the respective experimental values. It is important to mention that electronic and geometrical parameters of these species in solution are crucial for understanding many reactions and processes related to the environment. Our approach can provide important insights about systems of increasing complexity as those related to the adsorption on minerals, complexation and nucleation modeling, and the pK_a determination of mineral surfaces.

Acknowledgment. This work has been supported by the Brazilian Research Agencies: Conselho Nacional para o Desenvolvimento Científico e Tecnológico (CNPq), Coordenação de Aperfeiçoamento de Pessoal de Ensino Superior (CAPES), and Fundação de Amparo à Pesquisa do Estado de Minas Gerais (FAPEMIG). The Millennium Science Initiative: Water a

Mineral Approach and PRONEX-FAPEMIG (EDT 2403/03) are also gratefully acknowledged.

References and Notes

(1) Bernhard, M.; Brinckman, F. E.; Sadler, P. J. *The Importance of Chemical Speciation in Environmental Processes*; Springer-Verlag: Berlin, Germany, 1986.

(2) Sigel, H. *Metal Ions in Biological Systems*; Marcel Dekker: New York, 1982; Vol. 14.

(3) Dhungana, S.; Ratledge, C.; Crumbliss, A. L. *Inorg. Chem.* **2004**, *43*, 6274.

(4) Osseo-Asare, K.; Zeng, X. *Int. J. Miner. Process.* **2000**, *58*, 319.

(5) Pullin, M. J.; Cabaniss, S. E. *Geochim. Cosmochim. Acta* **2003**, *67*, 4067.

(6) Moses, C. O.; Nordstrom, D. K.; Herman, J. S.; Mills, A. L. *Geochim. Cosmochim. Acta* **1987**, *51*, 1561.

(7) Caldeira, C. L.; Ciminelli, V. S. T.; Dias, A.; Osseo-Asare, K. *Int. J. Miner. Process.* **2003**, *72*, 373.

(8) Zeng, X.; Osseo-Asare, K. *Colloids Surf. A* **2001**, *177*, 247.

(9) Rosso, K. M.; Smith, D. M. A.; Dupuis, M. *J. Phys. Chem. A* **2004**, *108*, 5242.

(10) Harris, D.; Loew, G. H.; Komornicki, A. *J. Phys. Chem. A* **1997**, *101*, 3959.

(11) Kallies, B.; Meier, R. *Inorg. Chem.* **2001**, *40*, 3101.

(12) Martin, R. L.; Hay, P. J.; Pratt, L. R. *J. Phys. Chem. A* **1998**, *102*, 3565.

(13) Koester, A. M.; Flores, R.; Geudtner, G.; Goursot, A.; Heine, T.; Patchkovskii, S.; Reveles, J. U.; Vela, A.; Salahub, D. *Program deMon*, version 1.1.0; NRC: Ottawa, Canada, 2004.

(14) Becke, A. D. *Phys. Rev. A: At., Mol., Opt. Phys.* **1988**, *38*, 3098.

(15) Perdew, J. P. *Phys. Rev. B: Condens. Matter* **1986**, *33*, 8822.

(16) Perdew, J. P.; Burke, K.; Ernzerhof, M. *Phys. Rev. Lett.* **1996**, *77*, 3865.

(17) Godbout, N.; Salahub, D. R.; Andzelm, J.; Wimmer, E. *Can. J. Chem. Rev.* **1992**, *70*, 560.

(18) Schafer, A.; Horn, H.; Ahlrichs, R. *J. Chem. Phys.* **1992**, *97*, 2571.

(19) Krack, M.; Koster, A. M. *J. Chem. Phys.* **1998**, *108*, 3226.

(20) Koster, A. M.; Flores-Moreno, R.; Reveles, J. U. *J. Chem. Phys.* **2004**, *121*, 681.

(21) Fletcher, R. *Comput. J.* **1970**, *13*, 317.

(22) Broyden, C. G. *J. Inst. Math. Its Appl.* **1970**, *6*, 76.

(23) Goldfarb, D. *Math. Comput.* **1970**, *24*, 23.

(24) Shanno, D. F. *Math. Comput.* **1970**, *24*, 647.

(25) Broyden, C. G. *J. Inst. Math. Its Appl.* **1970**, *6*, 222.

(26) McQuarrie, D. A.; Simon, J. D. *Molecular Thermodynamics*; University Science Books: Sausalito, CA, 1999.

(27) Cossi, M.; Barone, V.; Cammi, R.; Tomasi, J. *Chem. Phys. Lett.* **1996**, *255*, 327.

(28) Tomasi, J.; Persico, M. *Chem. Rev.* **1994**, *94*, 2027.

(29) Frisch, M. J.; Trucks, G. W.; Schlegel, H. B.; Scuseria, G. E.; Robb, M. A.; Cheeseman, J. R.; Zakrzewski, V. G.; Montgomery, J. A., Jr.; Stratmann, R. E.; Burant, J. C.; Dapprich, S.; Millam, J. M.; Daniels, A. D.; Kudin, K. N.; Strain, M. C.; Farkas, O.; Tomasi, J.; Barone, V.; Cossi, M.; Cammi, R.; Mennucci, B.; Pomelli, C.; Adamo, C.; Clifford, S.; Ochterski, J.; Petersson, G. A.; Ayala, P. Y.; Cui, Q.; Morokuma, K.; Malick, D. K.; Rabuck, A. D.; Raghavachari, K.; Foresman, J. B.; Cioslowski, J.; Ortiz, J. V.; Stefanov, B. B.; Liu, G.; Liashenko, A.; Piskorz, P.; Komaromi, I.; Gomperts, R.; Martin, R. L.; Fox, D. J.; Keith, T.; Al-Laham, M. A.; Peng, C. Y.; Nanayakkara, A.; Gonzalez, C.; Challacombe, M.; Gill, P. M. W.; Johnson, B. G.; Chen, W.; Wong, M. W.; Andres, J. L.; Head-Gordon, M.; Replogle, E. S.; Pople, J. A. *Gaussian 98*, revision A.6; Gaussian, Inc.: Pittsburgh, PA, 1998.

(30) Saracino, G. A. A.; Improta, R.; Barone, V. *Chem. Phys. Lett.* **2003**, *373*, 411.

(31) Barone, V.; Cossi, M.; Tomasi, J. *J. Chem. Phys.* **1997**, *107*, 3210.

(32) Amira, S.; Spangberg, D.; Probst, M.; Hermansson, K. *J. Phys. Chem. B* **2004**, *108*, 496.

(33) Amira, S.; Spangberg, D.; Zelin, V.; Probst, M.; Hermansson, K. *J. Phys. Chem. B* **2005**, *109*, 14235.

(34) Chang, C. M.; Wang, M. K. *Chem. Phys. Lett.* **1998**, *286*, 46.

(35) D'Angelo, P.; Benfatto, M. *J. Phys. Chem. A* **2004**, *108*, 4505.

(36) Herdman, G. J.; Neilson, G. W. *J. Phys.: Condens. Matter* **1992**, *4*, 627.

(37) Jarzecki, A. A.; Anbar, A. D.; Spiro, T. G. *J. Phys. Chem. A* **2004**, *108*, 2726.

(38) Ohtaki, H.; Radnai, T. *Chem. Rev.* **1993**, *93*, 1157.

(39) Rustad, J. R.; Dixon, D. A.; Rosso, K. M.; Felmy, A. R. *J. Am. Chem. Soc.* **1999**, *121*, 3234.

(40) Brunschwig, B. S.; Creutz, C.; Macartney, D. H.; Sham, T. K.; Sutin, N. *Faraday Discuss.* **1982**, 113.

(41) Kubicki, J. D. *J. Phys. Chem. A* **2001**, *105*, 8756.

(42) Bauschlicher, C. W.; Langhoff, S. R. *Int. Rev. Phys. Chem.* **1990**, *9*, 149.

(43) Sahoo, N.; Das, T. P. *J. Chem. Phys.* **1989**, *91*, 7740.

(44) Langhoff, S. R.; Bauschlicher, C. W. *Ann. Rev. Phys.Chem.* **1988**, *39*, 181.

(45) Li, J.; Fisher, C. L.; Chen, J. L.; Bashford, D.; Noodleman, L. *Inorg. Chem.* **1996**, *35*, 4694.

(46) Lopes, L.; Laat, J.; Legube, B. *Inorg. Chem.* **2002**, *41*, 2505.

(47) Martin, R. B. *J. Inorg. Biochem.* **1991**, *44*, 141.

(48) De Abreu, H. A.; De Almeida, W. B.; Duarte, H. A. *Chem. Phys. Lett.* **2004**, *383*, 47.

(49) Schuurmann, G.; Cossi, M.; Barone, V.; Tomasi, J. *J. Phys. Chem. A* **1998**, *102*, 6706.

(50) Liptak, M. D.; Shields, G. C. *Int. J. Quantum Chem.* **2001**, *85*, 727.

(51) Liptak, M. D.; Shields, G. C. *J. Am. Chem. Soc.* **2001**, *123*, 7314.

(52) Toth, A. M.; Liptak, M. D.; Phillips, D. L.; Shields, G. C. *J.Chem. Phys.* **2001**, *114*, 4595.

(53) da Silva, C. O.; da Silva, E. C.; Nascimento, M. A. C. *J. Phys. Chem. A* **1999**, *103*, 11194.

(54) Liptak, M. D.; Gross, K. C.; Seybold, P. G.; Feldgus, S.; Shields, G. C. *J. Am. Chem. Soc.* **2002**, *124*, 6421.

(55) Silva, C. O.; da Silva, E. C.; Nascimento, M. A. C. *J. Phys. Chem. A* **2000**, *104*, 2402.

(56) Martell, A. E.; Smith, R. M.; Motekaitis, R. J. *NIST: Critically Selected Stability Constants of Metal Complexes*, 5th ed.; Texas A & M University: College Station, TX, 1997; pp NIST Standard Reference Database 46.

(57) Pliego, J. R. *Chem. Phys. Lett.* **2003**, *367*, 145.

(58) Tsuzuki, S.; Lüthi, H. P. *J. Chem. Phys.* **2001**, *114*, 3949.